International Journal of Environmental Science and Technology (2019) 16:7555–7564
https://doi.org/10.1007/s13762-019-02484-3

ORIGINAL PAPER

Bio-decolorization and novel bio-transformation of methyl orange by brown-rot fungi

A. S. Purnomo[1] · V. T. Mauliddawati[1] · M. Khoirudin[1] · A. F. Yonda[1] · R. Nawfa[1] · S. R. Putra[1]

Received: 11 April 2019 / Revised: 8 July 2019 / Accepted: 17 July 2019 / Published online: 27 July 2019

Abstract

An investigation was conducted to assess the ability of three species of brown-rot fungi to decolorize and transform methyl orange dye. Methyl orange was decolorized in a potato dextrose agar medium by *Fomitopsis pinicola*, *Gloeophyllum trabeum*, and *Daedalea dickinsii* at different concentrations of 50, 75, and 100 mg L^{-1}. Based on the values of the decolorization index, the highest methyl orange decolorization was found approximately 91% by *F. pinicola*, followed by *D. dickinsii* and *G. trabeum* of 82% and 76%, respectively, at a concentration of 50 mg L^{-1}. *F. pinicola* had the highest methyl orange transformation with percent decolorization values of approximately 97%, followed by *D. dickinsii* and *G. trabeum* of 93% and 67%, respectively, after a 14-day incubation period in potato dextrose broth. *F. pinicola* transformed methyl orange into six metabolic products: compounds **3**, **6**, **7**, **8**, **9**, and **10**, while *G. trabeum* transformed methyl orange into five metabolic products: compounds **1**, **2**, **3**, **4**, and **5**. Among brown-rot fungi, *D. dickinsii* had more metabolic products, with compounds **3**, **4**, **6**, **11**, **12**, **13**, **14**, **15**, **16**, **17**, and **18**. Based on the identification of metabolic products, novel bio-transformation was proposed that brown-rot fungi initially transformed methyl orange via three pathways: (1) demethylation, (2) desulfonylation, and (3) hydroxylation. This study indicated that brown-rot fungi can be used to decolorize and transform methyl orange dye as well as proposed novel bio-transformation of methyl orange by brown-rot fungi.

Keywords Biodegradation · Dye · *Fomitopsis pinicola* · *Gloeophyllum trabeum* · *Daedalea dickinsii*

Introduction

The production of synthetic dyes has increased with the progression of consumerism, with most being used in textile industries. It was estimated that approximately 10–15% of dyes do not bind to the fibers during the coloring process and are therefore discharged into the environment (Camargo and Morales 2013). Azo dyes are the most important synthetic dyes, containing at least one azo group as the color-producing group, attached to substituted benzene or naphthalene rings. Azo dyes are classified as the most recalcitrant, persistent, and resistant dyes to the degradative environmental activities because of their chemical stability and versatility (Gutowska et al. 2007; Thao et al. 2013; Saroj et al. 2014). Apart from causing esthetic problems, most azo dyes have substantial toxic effects to the environment as well as humans. Methyl orange (MO) has been reported as a type of azo dye that is soluble in water, easily absorbed into the skin and inhaled, as well as a potential mutagenic and carcinogenic agent (Rafii et al. 1997; Wu et al. 2008; Sudha et al. 2014). Since the discovery of the harmful effects of MO (Shah et al. 2013; Bazrafshan et al. 2014; Grizca and Setyo 2018), a process of degradation of this dye is now required.

Some chemical and physical methods have been used and developed for the degradation of azo dyes, such as reductive degradation (Bigg and Judd 2001; Bokare et al. 2008), ozonation (Liakou et al. 1997; Yildirim et al. 2011), adsorption (Abramian and El-Rassy 2009; Roy et al. 2013), electrochemical (Ramirez et al. 2013), photocatalysis (Chen et al. 2011; Singla et al. 2014), and the Fenton reaction (Chacón et al. 2006; Peternel et al. 2007; Gomathi et al. 2009). The Fenton reaction is an effective technology with a catalytic oxidation process using hydrogen peroxide (H_2O_2) and ferrous ions (Fe^{2+}) mixtures to produce hydroxyl radicals

Editorial responsibility: J Aravind.

✉ A. S. Purnomo
adi_setyo@chem.its.ac.id

[1] Department of Chemistry, Faculty of Science, Institut Teknologi Sepuluh Nopember (ITS), Kampus ITS Sukolilo, Surabaya 60111, Indonesia

(·OH) as the current strongest oxidant known in biological systems for the destruction of a large number of hazardous and organic pollutants (Fenton 1894; Koenigs 1974; Wood 1994; Zhu et al. 2014). The treatment of azo dyes using the Fenton reaction has been reported previously (Chacón et al. 2006; Peternel et al. 2007; Gomathi et al. 2009); however, this method has a relatively high cost in practice and has the potential to destroy other environmental substances.

Biodegradation using microorganisms, especially fungi, is one of the most effective, cheap, and environmentally friendly methods for degrading some pollutants—including dyes (Purnomo 2017). Brown-rot fungi (BRF) have the biological Fenton reaction capable of generating hydroxyl radicals (·OH) that are able to degrade cellulose and hemicellulose effectively, as well as several xenobiotic compounds, such as 2,4,6-trinitrotoluene (Newcombe et al. 2002), chlorophenol (Schlosser et al. 2000), fluoroquinolone antibiotics (Wetzstein et al. 1997; 1999), aldrin and dieldrin (Purnomo et al. 2017a), DDT (Purnomo et al. 2017b; Sariwati et al. 2017; Sariwati and Purnomo 2018; Setyo et al. 2018), and dyes (Gomaa et al. 2010; Rizqi and Purnomo 2017). In our previous studies, three species of BRF, namely *Fomitopsis pinicola*, *Gloeophyllum trabeum*, and *Daedalea dickinsii* showed the greatest abilities in degrading DDT in liquid media (Purnomo et al. 2008; 2010c) as well as in contaminated soil (Purnomo et al. 2011a), with the Fenton reaction being used in the degradation mechanism (Purnomo et al. 2011b). In the current study, the ability of these BRF in degrading MO was investigated and compared with the characterization of the major metabolic products, and clarification of the degradation pathway also included. This was the first report on the bio-transformation of MO by BRF.

Materials and methods

Chemicals

Methyl orange (MO, $C_{14}H_{14}N_3NaO_3S$, molecular weight 327.34 g mol^{-1}) was purchased from SAP Chemicals, while methanol, *n*-hexane, acetone, and *N*,*N*-dimethylformamide (DMF) were purchased from Wako Pure Chemical Industries (Osaka, Japan).

Fungi

The brown-rot fungi used in this study were *F. pinicola* NBRC8705, *G. trabeum* NBRC6509, and *D. dickinsii* NBRC31163 (NITE Biological Resource Center, NBRC; Chiba, Japan). These fungi were maintained on potato dextrose agar (PDA; Difco, Detroit, MI, USA) incubated at 30 °C as stock cultures.

Decolorization of MO in solid agar media

PDA was used for the solid agar media test, which had a varying MO concentration (0, 50, 75, and 100 mg mL^{-1}, Jayasinghe et al. 2008). The mycelium of BRF (diameter 1 cm) were inoculated into the PDA medium containing MO and then incubated at 30 °C for 14 days. The mycelium (DM) diameter growth and the zone of color change (ZCC) on the agar plates were measured after the incubation period. The ability of BRF to decolorize MO was determined as the decolorization index (DI) using the following equation:

$$\mathrm{DI} = \left(\frac{\mathrm{ZCC}}{\mathrm{DM}}\right) \times 100\%$$

Biodegradation of MO in liquid media

The biodegradation of MO using BRF in PDB medium was performed in vivo. One plug (diameter 1 cm) of mycelia of stock cultures of BRF from a PDA plate was inoculated into 10 mL of potato dextrose broth (PDB; Difco, Detroit, MI, USA) in a 100-mL Erlenmeyer flask, which pre-incubated statically at 30 °C for 7 days.

After pre-incubation for 7 days, MO (final concentration: 50 mg L^{-1}) was added to the cultures and incubated at 30 °C. The degradation of MO was monitored after 0, 7, and 14 days of treatments. The cultures were placed in 15-mL Falcon tubes and centrifuged at 4000 rpm for 10 min to obtain the biomass and supernatant, measured using a spectrometer UV–VIS at wavelength 400–650 nm in which the max wavelength of MO was 465 nm, while the rest were stored for metabolite product identification. For control, the cultures were performed without the addition of BRF. Percent degradation was calculated based on the equation:

$$\%\ \text{decolorization (PD)} = \frac{\mathrm{Abs}_0 - \mathrm{Abs}_t}{\mathrm{Abs}_0} \times 100\%$$

where Abs_0 and Abs_t are control and treatment absorbances, respectively.

Identification of metabolic products

The supernatant was analyzed using liquid chromatography–time-of-flight–mass spectrometry (LC–ToF–MS) to determine the metabolite products, and the electrospray ionization (ESI) had a mass range of 50–500 m/z. The column used was AcclaimTM RSLC 120 C18 2.1 × 100 mm with a particle size of 2.2 µm. The mobile phase was methanol to water at a ratio of 99:1 for 3 min, with a speed flow rate of 0.2 mL min^{-1} and 61:39 for 7 min with a rate of 0.4 mL min^{-1}.

Statistical analysis

The results are presented as the average of triplicate measurements. Any statistically significant differences between or within groups during the MO transformation were determined by the *t* test, which a confidence level of 5% ($P < 0.05$) (Purnomo et al. 2010a; b, 2013, 2014).

Results and discussion

The Fenton chemical reaction had been used as an effective method for decolorizing azo dyes (Chacón et al. 2006; Peternel et al. 2007; Gomathi et al. 2009); however, it is relatively expensive and considered destructive to other environmental substances. Therefore, the biological Fenton reaction from BRF may be useful as a cheaper, environmentally friendly method. Previously, *F. pinicola*, *G. trabeum*, and *D. dickinsii* had been reported for their ability to degrade DDT by involving the Fenton reaction (Purnomo et al. 2008; 2010c; 2011a). In this study, bio-decolorization and bio-transformation of MO by these BRF were investigated and compared.

The decolorization of MO by BRF on a PDA medium was evaluated using PDA's agar plate containing MO in different concentrations (final concentration 50, 75, 100 mg L^{-1}), which was used as the initial screen to verify whether BRF could decolorize MO, as well as to determine its optimal concentration. The concentration of MO below 50 mg L^{-1} and above 100 mg L^{-1} produced vague and thick colors, respectively, thus making observation quite difficult. Previously, the same various concentrations (final concentration 50, 75, 100 mg L^{-1}) were used to evaluate the decolorization of methylene blue (MB) by brown-rot fungus *D. dickinsii* (Rizqi and Purnomo 2017). The diameter growth mycelium (DM) and the zone of color change (ZCC) were used to evaluated the decolorization index (DI) that defines the ability of BRF in decolorizing MO. Based on the DM values, every tested BRF did not show a significant difference ($P < 0.05$) in growth in the PDA medium containing MO in all variation concentrations, except *G. trabeum* which grew in PDA containing 100 mg L^{-1} (Table 1). Through comparing the control medium (PDA without addition MO), it was found that the growth of all BRF did not show any significant differences (Table 1), indicating that MO was not toxic for BRF. Vasdev (2011) reported that the growth of six species of white-rot fungi (WRF) was not affected by the presence of dyes in the medium, implying that some fungi are able to tolerate and decolorize dyes for growth. *Pycnoporus coccineus*, *Fomes fomentarius*, *Stereum ostrea*, *and Pycnoporus cinnabarinus* have good mycelial growth in a medium containing MB, but they could not degrade methylene blue (MB) (Jayasinghe et al. 2008).

During a 5-day incubation period, the color of MO (orange) changed to red as a result of changes in the structure. These changes occurred due to variations in the pH of the PDA medium, which became acidic (Del Nero et al. 2005). It has been known in advance that the BRF produces some organic acids, such as oxalic acid (Takao 1965; Espejo and Agosin 1991). The low pH encouraged BRF to produce hydroxyl radical from the Fenton reaction (Akamatsu et al. 1992; Dutton and Evans 1996). After the 5-day incubation period, the red color began to decolorize. *G. trabeum*

Table 1 Decolorization of MO by BRF in PDA medium at various concentrations of MO during 14-day incubation period at 30 °C

MO concentration (mg L^{-1})	Diameter mycelium (DM) (cm)	Zone of color change (ZCC) (cm)	Decolorization Index (DI) (%)
G. trabeum			
Control (without MO)	8.15 ± 0.07a		
50	8.03 ± 0.06a	6.07 ± 0.06a	75.52 ± 0.65a
75	8.17 ± 0.06a	5.73 ± 0.06b	70.21 ± 1.21b
100	8.07 ± 0.06b	4.53 ± 0.12c	56.19 ± 1.03c
D. dickinsii			
Control (without MO)	8.20 ± 0.01c		
50	7.77 ± 0.06c	6.04 ± 0.36d	82.38 ± 4.07d
75	8.03 ± 0.12c	6.13 ± 0.40d	76.4 ± 5.96d
100	7.87 ± 0.12c	4.33 ± 0.29e	55.13 ± 4.44e
F. pinicola			
Control (without MO)	8.10 ± 0.14d		
50	7.43 ± 0.67d	6.77 ± 0.80f	90.97 ± 5.80f
75	8.03 ± 0.29d	7.12 ± 0.25f	88.64 ± 3.38f
100	7.57 ± 0.55d	6.40 ± 0.35f	84.66 ± 1.61f

Data are presented as the mean ± standard deviations ($n = 3$). Data followed by the different lower letter on each column indicated significant difference among fungal inoculum at various concentration of MO ($P < 0.05$)

showed significant differences in decolorizing MO in various concentrations: the higher the concentration of MO, the lower the obtained decolorized zone was (Table 1). The highest decolorized zone was shown at an MO concentration of 50 mg L^{-1}; however, *F. pinicola* did not show a significant difference in decolorizing, as well as *D. dickinsii* except at 100 mg L^{-1} concentration where it showed the lowest one (Table 1).

The ID values of each BRF in different concentrations of MO are shown in Table 1. In general, the higher MO concentration in the PDA medium, the lower the ID values obtained. *G. trabeum* showed significant differences in ID values of approximately 76, 70, and 56% in MO concentrations of 50, 75, and 100 mg L^{-1}, respectively (Table 1). *D. dickinsii* did not show significant differences in the ID values except at an MO concentration of 100 mg L^{-1} that showed the lowest ones. *F. pinicola* also did not show significantly different ID values in all variation of MO concentration. These results indicate that at higher concentrations, BRF needs more activity to decolorize MO. In general, an MO concentration of 50 mg L^{-1} showed the highest BRF ID values, with *F. pinicola* showing the best BRF to decolorize MO with approximately 91% ID, followed by *D. dickinsii* and *G. trabeum* of 82% and 76%, respectively. Previously, *D. dickinsii* could decolorize MB with the highest ID value (92%) at 50 mg L^{-1} of MB (Rizqi and Purnomo 2017). Zeng et al. (2015) reported the same trend indicating that dye concentration has a negative effect on the decolorization percentage. It is assumed that high concentrations of dye result in slower decolorization rates. The *Kocuria rosea* (MTCC 1532) bacterium showed 100% decolorization of the MO (50 mg L^{-1}) medium containing yeast extract (Parshetti et al. 2010), while *Aeromonas* sp. DH-6 reached nearly 100% decolorization of MO (100 mg L^{-1}) after a 12 h incubation (Du et al. 2015). Based on this screening, 50 mg L^{-1} was selected as the concentration of MO in the liquid medium test.

Figure 1 illustrates the absorbance profile of MO during degradation by BRF, when MO was added to the pre-culture of all BRF (0 day), the absorbance of MO was decreased, and the orange color changed to red, indicating a transformation in structure due to the acid condition, where organic acids were formed during the pre-incubation of BRF. Besides producing organic acids, BRF may produce some secondary metabolites as well as the Fenton reaction to produce hydroxyl radicals during pre-incubation (Takao 1965; Espejo and Agosin 1991; Akamatsu et al. 1992; Dutton and Evans, 1996; Del Nero et al. 2005; Purnomo et al. 2008;

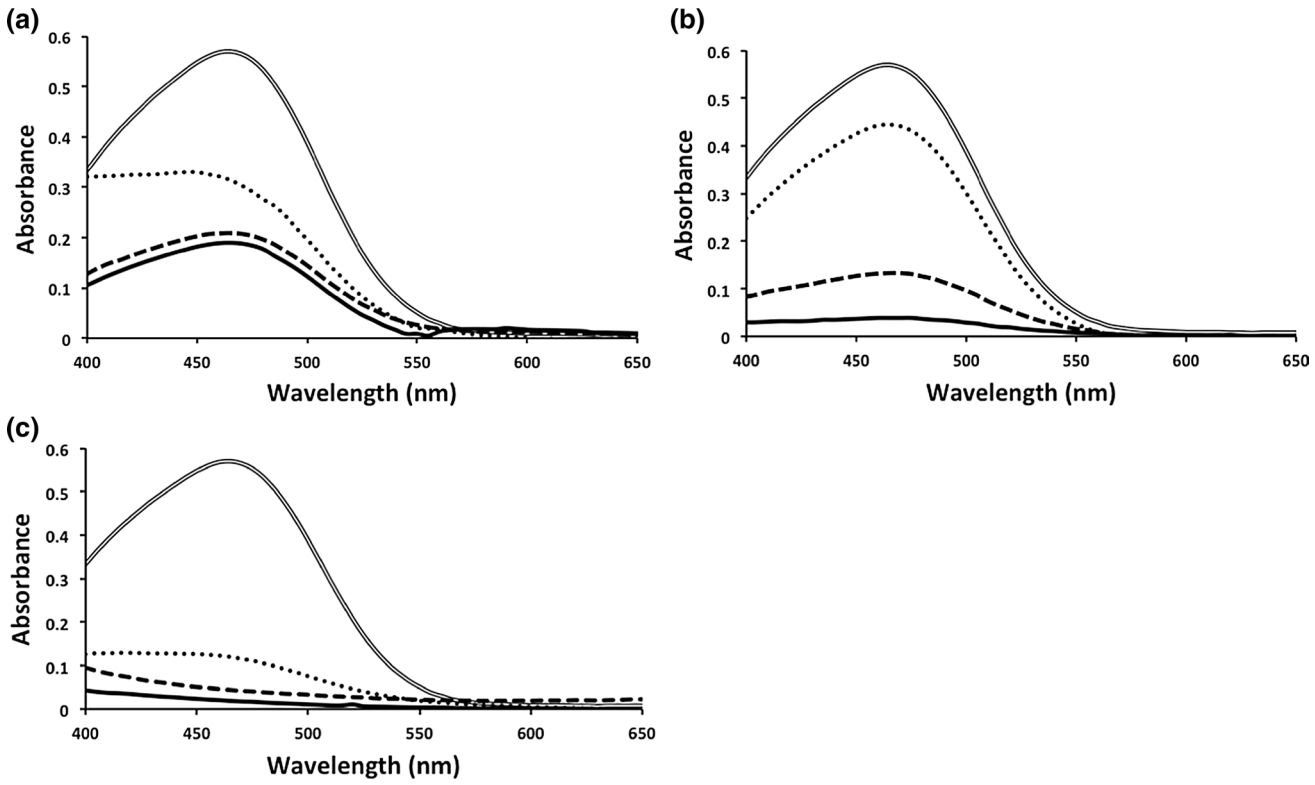

Fig. 1 Profile of bio-decolorization of MO by brown-rot fungi *G. trabeum* (**a**), *D. dickinsii* (**b**), and *F. pinicola* (**c**) in PDB medium at 0 (dot line), 7 (dashed line) and 14 (continuous line) days of incubation at 30 °C. Control (double line) was defined as cultures without the addition of fungi. Data are presented as the mean ($n=3$)

2010c; 2011a; Wahyuni et al. 2016). The results had a similar tendency in the degradation of MO in the PDA medium. Among BRF, the *F. pinicola* pre-culture showed the highest degradation at 0-day incubation, indicating that it is able to produce more organic acid or enzymes (Fig. 1c). On the other hand, the *D. dickinsii* pre-incubation culture showed the lowest degradation at 0-day incubation, suggesting that this fungus may produce a smaller amount of organic acids. During the degradation of MO for both 7 and 14 days, the MO absorbances were decreased slightly (Fig. 1), suggesting a degradation by BRF. The highest absorbance of MO was obtained at a wavelength of 465 nm, which was used to determine the degradation rate quantitatively by measuring percentage decolorization (PD).

Table 2 highlights the percentage decolorization (PD) and biomass dry weight of BRF during degradation. All of the BRF showed significant different weights, the longer the incubation times were, the higher the biomass was obtained. In each BRF, the higher biomass and PD values obtained indicated that biomass has a direct influence during MO degradation by the production of higher metabolic products or enzymes. *G. trabeum* showed the highest biomass, followed by *F. pinicola* and *D. dickinsii* of approximately 26, 25, and 23 mg, respectively, over the 14-day incubation period. *G. trabeum*, however, showed the lowest degradation rate at 67%, whereas *F. pinicola* showed the highest at 97% during the 14 days. This indicated that the quantity of biomass was not only the factor affecting the degradation rate, but also the type of fungus. Even

Table 2 Percentage decolorization of MO by BRF and its biomass dry weight in PDB medium at 30 °C during various time of incubation

Incubation time (days)	Biomass dry weight (mg)	Percent decolorization (PD)* (%)
G. trabeum		
0	18.1 ± 0.2a	44.90 ± 0.56a
7	19.4 ± 0.5b	63.33 ± 2.11b
14	26.2 ± 0.1c	66.70 ± 0.31c
D. dickinsii		
0	5.9 ± 0.1d	21.96 ± 7.14d
7	14.5 ± 0.7e	76.67 ± 6.69e
14	22.9 ± 0.3f	93.16 ± 3.14f
F. pinicola		
0	13.3 ± 0.2g	82.40 ± 1.31
7	18.1 ± 0.1	93.55 ± 0.83a
14	24.7 ± 0.6i	97.21 ± 0.16

*The data were determined by UV–VIS spectrophotometer at 465 nm. Data are presented as the mean ± standard deviations ($n = 3$). Data followed by the different lower letters on each column indicated significant difference among fungal inoculum at various concentrations of MO ($P < 0.05$)

though the *F. pinicola* and *D. dickinsii* biomasses were lower than *G. trabeum* biomass, they had a higher ability to degrade MO. Generally, it was assumed that the ability of BRF to degrade MO may be associated with the ability to produce extracellular enzymes (Singh et al. 2015; Wahyuni et al. 2017) and hydroxyl radicals generated by the Fenton reaction (Purnomo et al. 2008, 2010a, 2011b) (Fig. 1). However, to confirm the involvement of extracellular enzymes and the Fenton reaction in the degradation process, further investigation is needed.

LC–TOF/MS analysis showed that each BRF produced different metabolic products (Table 3), with most transforming MO via demethylation and hydroxylation as the main reaction. *G. trabeum* transformed MO into five metabolic products, namely 4-{[3-hydroxy-4-(methylamino)phenyl] diazenyl} benzenolate (*m/z* 242, compound **1**), 4-{[4-(methylideneamino)phenyl] diazenyl} benzenolate (*m/z* 255, compound **2**), 4-[(4-aminophenyl) diazenyl] benzene sulfonate (*m/z* 276, compound **3**), 4-{[4-(dimethylamino)-3-hydroxyphenyl] diazenyl} benzene sulfonate (*m/z* 320, compound **4**), and 4-[(4-amino-3,5-dihydroxyphenyl) diazenyl]-3-hydroxybenzene sulfonate (*m/z* 324, compound **5**). On the other hand, *F. pinicola* transformed MO into six metabolic products, namely 4-{[4-(dimethylamino) phenyl] diazenyl} benzenolate (*m/z* 240, compound **6**), 4-[(4-aminophenyl) diazenyl] benzene sulfonate (*m/z* 276, compound **3**), 4-[(4-amino-3-hydroxy phenyl) diazenyl] benzene sulfonate (*m/z* 292, compound **7**), 4-[(4-amino-3-hydroxy phenyl) diazenyl]-3-hydroxy benzene sulfonate (*m/z* 308, compound **8**), 4-{[3-hydroxy-4-(methylamino) phenyl] diazenyl}3-hydroxy benzene sulfonate (*m/z* 322, compound **9**), and 4-{[4-(dimethylamino)-3-hydroxy phenyl] diazenyl}-3-hydroxy benzene sulfonate (*m/z* 336, compound **10**). Among the BRF, *D. dickinsii* had more metabolic products and the hydroxylation was more dominant over demethylation. The metabolic products of MO by *D. dickinsii* were *N*,*N*-dimethyl-4-phenyl diazenylaniline (*m/z* 225, compound **11**), 4-{[4-(dimethylamino)phenyl] diazenyl} benzenolate (*m/z* 240, compound **6**), 4-(phenyldiazenyl) benzene sulfonate (*m/z* 261, compound **12**), 4-[(4-aminophenyl)diazenyl] benzene sulfonate (*m/z* 276, compound **3**), 4-{[4-(dimethylamino)-3-hydroxyphenyl]diazenyl} benzene sulfonate (*m/z* 320, compound **4**), 4-{[4-(dimethylamino)-3,5-dihydroxyphenyl]diazenyl} benzene sulfonate (*m/z* 336, compound **13**), 4-{[4-(dimethylamino)-2,3,5-trihydroxyphenyl]diazenyl} benzene sulfonate (*m/z* 352, compound **14**), -{[4-(dimethylamino)-2,3,5-trihydroxyphenyl]diazenyl}-3-hydroxybenzene sulfonate (*m/z* 368, compound **15**), 4-{[4-(dimethylamino)-2,3,5-trihydroxyphenyl]diazenyl}-2,5-dihydroxybenzene sulfonate (*m/z* 384, compound **16**), 4-{[4-(dimethylamino)-2,3,5-trihydroxyphenyl]diazenyl}-2,3,5-trihydroxybenzene sulfonate (*m/z* 400, compound **17**), and

Table 3 Metabolite products of MO degradation by brown-rot fungi

RT (min)	Mr	Name	Fragmentation	Structure
G. trabeum				
2.6	225	4-{[4-(methylamino) phenyl] diazenyl} benzenolate **(2)**	225[M^+], 209 [M^+-O], 179 [209-$NHCH_3$], 103 [179-C_6H_4], 75[103-N_2]	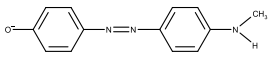
4.2	324	4- [(4- amino- 3,5- dihydroxy phenyl) diazenyl]- 3- hydroxy benzene sulfonate **(5)**	324[M^+], 244[M^+-SO_3], 228[244-NH_2], 136[228-C_6H_4O], 102[136-$(OH)_2$]	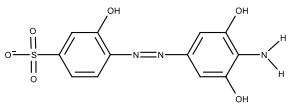
5.4	242	4- {[3- hydroxy- 4- (methylamino) phenyl] diazenyl} benzenolate **(1)**	242[M^+], 212[M^+-CH_3NH], 120[212-C_6H_4O], 103[120-OH]	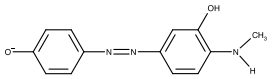
6.0	320	4- {[4- (dimethylamino)- 3- hydroxyphenyl] diazenyl} benzene sulfonate **(4)**	320[M^+], 240 [M^+-SO_3], 223 [240-OH], 193[223-$(CH_3)_2$], 179[193-N]	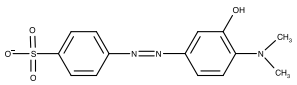
12.0	276	4- [(4- aminophenyl) diazenyl] benzene sulfonate **(3)**	276[M^+], 196[M^+-SO_3], 180[196-NH_2], 104[180-C_6H_4]	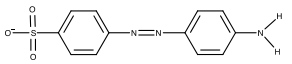
D. dickinsii				
1.7	261	4-(phenyldiazenyl) benzene sulfonate **(12)**	261[M^+], 170 [M^+-C_6H_5N], 76[170-SO_3N]	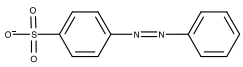
1.9	276	4-[(4-aminophenyl) diazenyl] benzene sulfonate **(3)**	276[M^+], 260 [M^+-NH_2],170 [M+-C_6H_5N], 76[170-SO_3N]	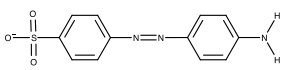
2.9	225	N,N-dimethyl-4-phenyl diazeny laniline **(11)**	225[M^+], 148 [M^+-C_6H_5], 120 [148-N_2], 105 [119-CH_3], 92[104-CH_3]	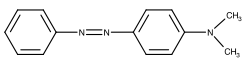
3.0	240	4- {[4- (dimethylamino) phenyl] diazenyl} benzenolate **(6)**	240[M^+], 134 [M^+-C_6H_4NO], 119 [134-CH_3], 104 [119-CH_3], 90[104-N], 76[90-N]	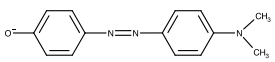
3.2	320	4- {[4- (dimethylamino)- 3- hydroxyphenyl] diazenyl} benzene sulfonate **(4)**	320[M^+], 240 [M^+-SO_3], 223 [240-OH], 193[223-$(CH_3)_2$], 179[193-N]	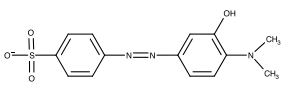
3.8	336	4- {[4- (dimethylamino)- 3,5- dihydroxyphenyl] diazenyl} benzene sulfonate **(13)**	336[M^+], 256 [M^+-SO_3], 239 [256-OH], 222 [239-OH], 192[222-$(CH_3)_2$], 178[192-N]	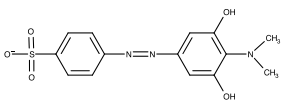
4.0	352	4- {[4- (dimethylamino)- 2,3,5- trihydroxyphenyl] diazenyl} benzene sulfonate **(14)**	352[M^+], 272[M^+-SO_3], 228[272-N$(CH_3)_2$], 152[228-C_6H_4], 138[152-N]	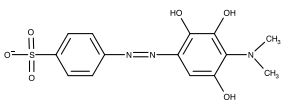

Table 3 (continued)

4.2	368	4- {[4- (dimethylamino)- 2,3,5- trihydroxyphenyl] diazenyl}- 3- hydroxy benzene sulfonate **(15)**	368[M^+], 317[M^+-$(OH)_3$], 273[317-$N(CH_3)_2$], 193[273-SO_3], 118[193-C_6H_3]	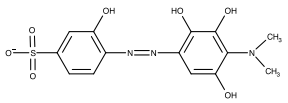
4.4	384	4- {[4- (dimethylamino)- 2,3,5- trihydroxyphenyl] diazenyl}- 2,5- dihydroxy benzene sulfonate **(16)**	384[M^+], 367[M^+-OH], 287 [367-SO_3], 243[287-$N(CH_3)_2$], 226[243-OH], 149[226-C_6H_4]	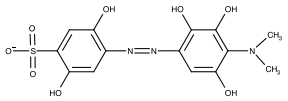
5.7	400	4- {[4- (dimethylamino)- 2,3,5- trihydroxyphenyl] diazenyl}- 2,3,5- trihydroxy benzene sulfonate **(17)**	400[M^+], 232 [M^+-$C_6H(OH)_3N(CH_3)_2$], 118 [232-$SO_3(OH)_2$]	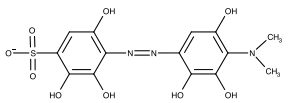
6.5	432	4- {[4- (dimethylamino)- 2,3,5,6- tetrahydroxyphenyl] diazenyl}- 2,3,5,6- tetrahydroxy benzene sulfonate **(18)**	432[M^+], 308 [M^+-$SO_3N(CH_3)_2$], 240 [308-$(OH)_4$], 206 [240-$(OH)_2$], 117[206-$C_6(OH)$]	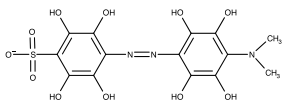
F. pinicola				
2.0	322	4- {[3- hydroxy- 4- (methylamino)phenyl] diazenyl}3-hydroxy benzene sulfonate **(9)**	322[M^+], 242 [M^+-SO_3], 225 [242-OH], 210[225-CH3], 195[210-NH]	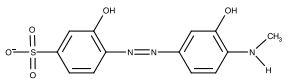
3.4	240	4- {[4- (dimethylamino) phenyl] diazenyl} benzenolate **(6)**	240[M^+], 134 [M^+-C_6H_4NO], 119 [134-CH_3], 104 [119-CH_3], 90[104-N], 76[90-N]	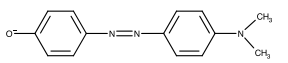
3.6	276	4- [(4- aminophenyl) diazenyl] benzene sulfonate **(3)**	276[M^+], 260 [M^+-NH_2],170 [M+-C_6H_5N], 76[170-SO_3N]	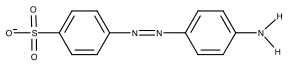
4.0	292	4- [(4- amino- 3- hydroxy phenyl) diazenyl] benzene sulfonate **(7)**	292[M^+], 212 [M^+-SO_3], 195 [212-OH], 179[195-NH2]	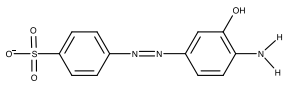
6.1	336	4- {[4- (dimethylamino)- 3- hydroxyphenyl] diazenyl}- 3- hydroxy benzene sulfonate **(10)**	336[M^+], 256 [M^+-SO_3], 239 [256-OH], 222 [239-OH], 192[222-$(CH_3)_2$], 178[192-N]	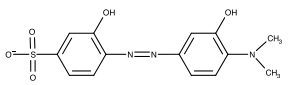
6.3	308	4- [(4- amino- 3- hydroxy phenyl) diazenyl]- 3- hydroxy benzene sulfonate **(8)**	308[M^+], 228 [M^+-SO_3], 211 [228-OH], 194 [211-OH], 178[194-NH_2]	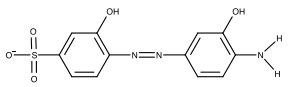

The data were determined by LCMS

4-{[4-(dimethylamino)-2,3,5,6-tetrahydroxyphenyl] diazenyl}-2,3,5,6-tetrahydroxybenzene sulfonate (*m/z* 432, compound **18**).

Some studies have reported that different mechanisms may be involved in the biodegradation of azo dyes such as enzymatic and non-enzymatic, as well as combinations of these mechanisms (Jadhav et al. 2008; Ayed et al. 2010). Among the enzymatic mechanisms, the involvement of laccase and azoreductase was often reported (Seesuriyachan et al. 2007; Parshetti et al. 2010; Ayed et al. 2010; Levin et al. 2012). Laccase is believed to be involved in the oxidation of the sulfonated side, while azoreductase is responsible for the reductive cleavage of the azo bridge (Jadhav et al. 2008; Ayed et al. 2010). Some metabolites (compounds **1**, **2**, **6**, **11**) were also detected as oxidation products of the sulfonated sides of MO, suggesting that laccase may be involved in the MO transformation by BRF. Some studies had reported laccase activity from *G. trabeum* (D'Souza et al. 1996), *D. dickinsii* (Mahmood et al. 2017), and *F. pinicola* (Park and Park 2014); however, since all of the identified metabolites of MO biodegradation by BRF were not products from the cleavage of the azo bridge, it is suggested that azoreductase is not involved in the MO biodegradation by BRF.

Based on the identification metabolites, MO degradation pathways were proposed (Fig. 2), by *G. trabeum* via three pathways: (1) demethylation to compound **3**, followed by hydroxylation to compound **5**, (2) desulfonylation that followed demethylation to compound **2**, hydroxylation to compound **1**, and (3) hydroxylation to compound **4**. Also, *F. pinicola* transformed MO via three pathways: (1) demethylation to compound **3**, followed by hydroxylation reactions to compounds **7** and **8**, (2) hydroxylation to compound **10**, followed by demethylation to compound **9**, and (3) desulfonylation to compound **6.** On the other hand, *D. dickinsii* also transformed MO via three pathways: (1) demethylation to compound **3,** followed by deamination to compound **12**, (2) desulfonylation to compound **6**, followed by reduction to compound **11**, and (3) hydroxylation to compound **4**, then followed by several hydroxylation to compounds **13**, **14**, **15**, **16**, **17**, and **18**. Thus, BRF initially transformed MO via three pathways: (1) demethylation, (2) desulfonylation, and (3) hydroxylation.

Conclusion

The present study clarified that BRF can decolorize and transform MO in PDA and PDB media. *F. pinicola* was concluded to be the best among BRF in decolorizing MO with DI by approximately 91% in the PDA medium and to transform MO with approximately 97% of PD in the PDB medium, after a 14-day incubation. Based on the identification of metabolic products, BRF initially transformed MO via three pathways: (1) demethylation, (2) desulfonylation, and (3) hydroxylation. This is the first report regarding MO

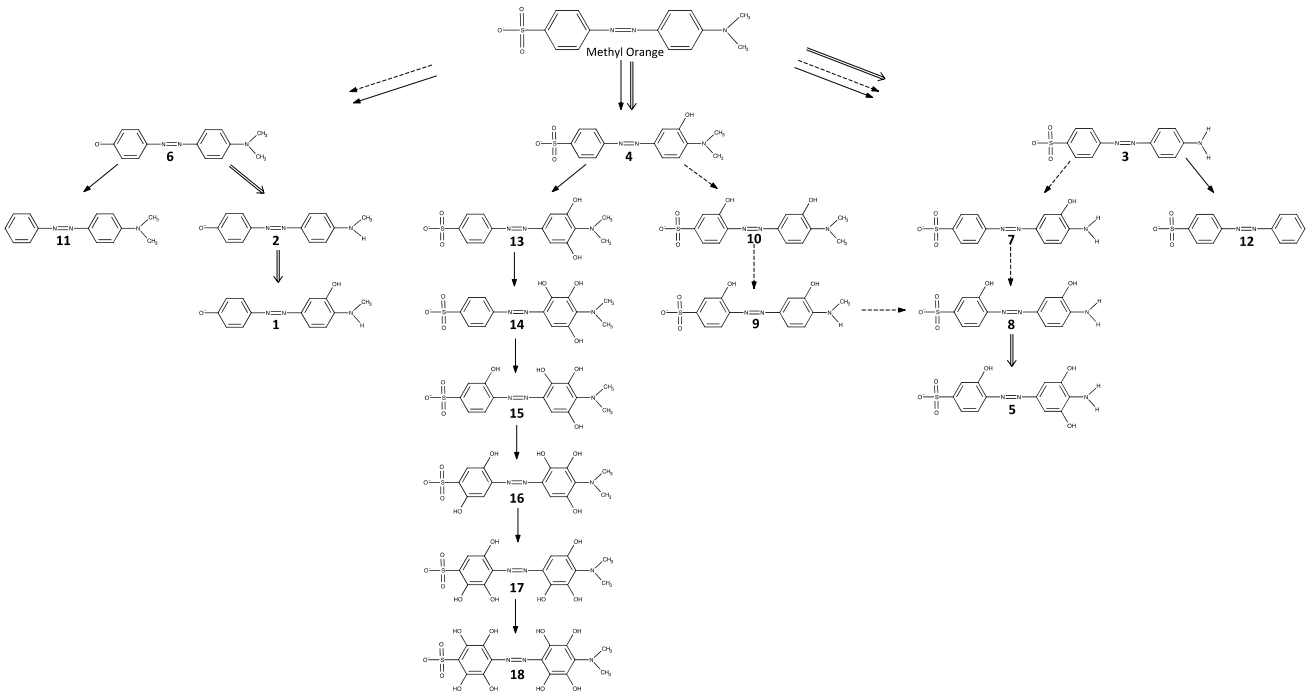

Fig. 2 Proposed MO bio-transformation pathway by brown-rot fungi *G. trabeum* (double line arrows), *D. dickinsii* (open arrows), and *F. pinicola* (dotted arrows)

transformation that indicates BRF can be used to decolorize and transform the MO dye.

Acknowledgements This work was supported by the competency-based research Grant No. 1/E/KPT/2018 from the Directorate General of Strengthening Research and Development, Ministry of Research, Technology and Higher Education, Indonesia.

References

Abramian L, El-Rassy H (2009) Adsorption kinetics and thermodynamics of azo-dye Orange II onto highly porous titania aerogel. Chem Eng J 150:403–410

Akamatsu Y, Takahashi M, Shimada M (1992) Cell-free extraction and assay of oxaloacetate from the brown-rot fungus *Tyromyces palustris*. Mokuzai Gakkaishi 38:495–500

Ayed L, Khelifi E, Jannet HB, Miladi H, Cheref A, Achour S, Bakhrouf A (2010) Response surface methodology for decolorization of azo dye Methyl Orange by bacterial consortium: produced enzymes and metabolites characterization. Chem Eng J 165:200–208

Bazrafshan E, Zarei AA, Nadi H, Zazouli MA (2014) Adsorptive removal of Methyl Orange dan Reactive Red 198 dyes by *Moringa peregrina* ash. Indian J Chem Techn 21:105–113

Bigg T, Judd S (2001) Kinetics of reductive degradation of azo dye by zero-valent iron. Process Saf Environ Prot 79(5):297–303

Bokare AD, Chikate RC, Rode CV, Paknikar KM (2008) Iron-nickel bimetallic nanoparticles for reductive degradation of azo dye Orange G in aqueous solution. Appl Catal B Environ 79(3):270–278

Camargo BCV, Morales MAM (2013) Azo dyes: characterization dan toxicity-A review. Text Light Indus Sci Techn (TLIST) 2:85–103

Chacón JM, Leal MT, Sánchez M, Bandala ER (2006) Solar photocatalytic degradation of azo-dyes by photo-Fenton process. Dyes Pigm 69(3):144–150

Chen C, Liu J, Liu P, Yu B (2011) Investigation of photocatalytic degradation of methyl orange by using nano-sized ZnO catalysts. Adv Chem Eng Sci 1(01):9–14

D'Souza TM, Boominathan K, Reddy CA (1996) Isolation of laccase gene-specific sequences from white rot and brown rot fungi by PCR. App Environ Microb 62(10):3739–3744

Del Nero J, de Araujo RE, Gomes ASL, de Melo CP (2005) Theoretical and experimental investigation of the second hyperpolarizabilities of methyl orange. J Chem Phys 122:104506

Du LN, Li G, Zhao YH, Xu HK, Wang Y, Zhou Y, Wang L (2015) Efficient metabolism of the azo dye methyl orange by *Aeromonas* sp. strain DH-6: characteristics and partial mechanism. Int Biodeterior Biodegrad 105:66–72

Dutton MV, Evans CS (1996) Oxalate production by fungi: its role in pathogenicity and ecology in the soil environment. Can J Microb 42:881–895

Espejo E, Agosin E (1991) Production and degradation of oxalic acid by brown rot fungi. App Environ Microbiol 57(7):1980–1986

Fenton HJH (1894) Oxidation of tartaric acid in presence of iron. J Chem Soc 65:899–910

Gomaa OM, Kareem H, Fatahy R (2010) Assessment of the efficacy of brown rot fungi in real textile waste water treatment. J Biotech 150:261

Gomathi DL, Girish KS, Mohan RK, Munikrishnappa C (2009) Photo degradation of methyl orange an azo dye by advanced Fenton process using zero valent metallic iron: influence of various reaction parameters and its degradation mechanism. J Hazard Mater 164(2–3):459–467

Grizca BE, Setyo PA (2018) Abilities of co-cultures of white-rot fungus *Ganoderma lingzhi* and bacteria *Bacillus subtilis* on biodegradation DDT. J Phys Conf Ser 1095:102015

Gutowska A, Czaplinska J, Jozwiak W (2007) Degradation mechanism of reactive Orange 113 dye by H_2O_2/Fe^{2+} and ozone in aqueous solution. Dyes Pigm 74:41–46

Jadhav SU, Kalme SD, Govindwar SP (2008) Biodegradation of Methyl red by *Galactomyces geotrichum* MTCC 1360. Int Biodeterior Biodegrad 62:135–142

Jayasinghe C, Imtiaj A, Lee GW, Im KH, Hur H, Yang HS, Lee TS (2008) Degradation of three aromatic dyes by white rot fungi and the production of ligninolytic enzymes. Mycobiology 36:114–120

Koenigs JW (1974) Hydrogen peroxide and iron: a proposed system for decomposition of wood by brown-rot basidiomycetes. Wood Fiber 6:66–80

Levin L, Grassi E, Carballo R (2012) Efficient azoic dye degradation by *Trametes trogii* and a novel strategy to evaluate products released. Int Biodeterior Biodegrad 75:214–222

Liakou S, Pavlou S, Lyberatos G (1997) Ozonation of azo dyes. Water Sci Technol 35(4):279–286

Mahmood RT, Asad MJ, Asgher M, Gulfraz M, Mukhtar T (2017) Analysis of lingolytic enzymes and decolorization of dispere violet S3RL, yellow brown S2RFL, red W4BS, yellow SRLP and red S3B by brown rot fungi. Pak J Agric Sci 54(2):407–413

Newcombe D, Paszcynsky A, Gajewska W, Kroger M, Feis G, Crawford R (2002) Production of small molecular weight catalyst and the mechanism of trinitrotoluene degradation by several *Gloeophyllum* species. Enzyme Microb Technol 30:506–517

Park N, Park SS (2014) Purification and characterization of a novel laccase from *Fomitopsis pinicola* mycelia. Int J Biol Macromol 70:583–589

Parshetti GK, Telke AA, Kalyani DC, Govindwar SP (2010) Decolorization and detoxification of sulfonated azo dye methyl orange by *Kocuria rosea* MTCC 1532. J Hazard Mater 176:503–509

Peternel IT, Koprivanac N, Božić AML, Kušić HM (2007) Comparative study of UV/TiO_2, UV/ZnO and photo-Fenton processes for the organic reactive dye degradation in aqueous solution. J Hazard Mater 148(1):477–484

Purnomo AS (2017) Microbe-assisted degradation of aldrin and dieldrin. In: Singh SN (ed) Microbe-induced degradation of pesticides, 1st edn. Springer, Basel, pp 1–22

Purnomo AS, Kamei I, Kondo R (2008) Degradation of 1,1,1-trichlro-2,2-bis (4-chlorophenyl) ethane (DDT) by brown-rot fungi. J Biosci Bioeng 105:614–621

Purnomo AS, Koyama F, Mori T, Kondo R (2010a) DDT degradation potential of cattle manure compost. Chemosphere 80(6):619–624

Purnomo AS, Mori T, Kamei I, Nishii T, Kondo R (2010b) Application of mushroom waste medium from *Pleurotus ostreatus* for bioremediation of DDT-contaminated soil. Int Biodeterior Biodegrad 64(5):397–402

Purnomo AS, Mori T, Kondo R (2010c) Involvement of Fenton reaction in DDT degradation by brown rot fungi. Int Biodet Biodeg 64:560–565

Purnomo AS, Mori T, Takagi K, Kondo R (2011a) Bioremediation of DDT contaminated soil using brown-rot fungi. Int Biodet Biodeg 65:691–695

Purnomo AS, Mori T, Kamei I, Kondo R (2011b) Basic studies and applications on bioremediation of DDT: a review. Int Biodet Biodeg 65(7):921–930

Purnomo AS, Mori T, Putra SR, Kondo R (2013) Biotransformation of heptachlor and heptachlor epoxide by white-rot fungus *Pleurotus ostreatus*. Int Biodet Biodeg 82:40–44

Purnomo AS, Putra SR, Shimizu K, Kondo R (2014) Biodegradation of heptachlor and heptachlor epoxide-contaminated soils by white-rot fungal inocula. Environ Sci Pollut Res 21:11305–11312

Purnomo AS, Nawfa R, Martak F, Shimizu K, Kamei I (2017a) Biodegradation of aldrin and dieldrin by the white-rot fungus *Pleurotus ostreatus*. Curr Microbiol 74(3):320–324

Purnomo AS, Ashari K, Hermansyah F (2017b) Evaluation of the synergistic effect of mixed cultures of white-rot fungus *Pleurotus ostreatus* and biosurfactant-producing bacteria on DDT biodegradation. J Microbiol Biotechnol 27(7):1306–1315

Rafii F, Hall JD, Cerniglia CE (1997) Mutagenicity of azo dyes used in foods, drugs and cosmetics before and after reduction by *Clostridium* species from the human intestinal tract. Food Chem Toxic 35(9):897–901

Ramirez C, Saldana A, Hernandez B, Acero R, Guerra R, Garcia-Segura S, Brillas E, Peralta-Hernandez JM (2013) Electrochemical oxidation of methyl orange azo dye at pilot flow plant using BDD technology. J Indus Eng Chem 19:571–579

Rizqi HD, Purnomo AS (2017) The ability of brown-rot fungus *Daedalea dickinsii* to decolorize and transform methylene blue dye. World J Microbiol Biotechnol 33(5):92

Roy A, Adhikari B, Majumder SB (2013) Equilibrium, kinetic, and thermodynamic studies of azo dye adsorption from aqueous solution by chemically modified lignocellulosic jute fiber. Ind Eng Chem Res 52(19):6502–6512

Sariwati A, Purnomo AS (2018) The effect of *Pseudomonas aeruginosa* addition on 1,1,1 Trichloro 2,2 bis (4 chlorophenyl) ethane DDT Biodegradation by Brown-Rot fungus *Fomitopsis pinicola*. Indones J Chem 18(1):75–81

Sariwati A, Purnomo AS, Kamei I (2017) Abilities of co-cultures of brown-rot fungus *Fomitopsis pinicola* and *Bacillus subtilis* on biodegradation DDT. Curr Microbiol 74:1068–1069

Saroj S, Kumar K, Pareek N, Prasad R, Singh RP (2014) Biodegradation of azo dyes Acid Red 183, Direct Blue 15 and Direct Red 75 by the isolate *Penicillium oxalicum* SAR-3. Chemosphere 107:240–248

Schlosser D, Fahr K, Karl W, Wetzstein HG (2000) Hydroxylated metabolites of 2,4-dichlorophenol imply a Fenton-type reaction in *Gloeophyllum striatum*. App Environ Microb 66:2479–2483

Seesuriyachan P, Takenaka S, Kuntiya A, Klayraung S, Murakami S, Aoki K (2007) Metabolism of azo dyes by *Lactobacillus casei* TISTR 1500 and effects of various factors on decolorization. Water Res 41:985–992

Setyo PA, Dwi RH, Sri F, Sulistyo PH, Ichiro K (2018) Effects of bacterium *Ralstonia pickettii* addition on DDT biodegradation by *Daedalea dickinsii*. Res J Chem Environ 22(Special issue II):151–156

Shah MP, Patel KA, Darji A (2013) Microbial degradation and decolorization of methyl Orange dye by an application of *Pseudomonas* spp. ETL-1982. Int J Environ Bioremediat Biodegrad 1:26–36

Singh RL, Singh PK, Singh RP (2015) Enzymatic decolorization and degradation of azo dyes-a review. Int Biodeterior Biodegrad 104:21–31

Singla P, Sharma M, Pandey OP, Singh K (2014) Photocatalytic degradation of azo dyes using Zn-doped and undoped TiO_2 nanoparticles. Appl Phys A 116(1):371–378

Sudha M, Saranya A, Selvakumar G, Sivakumar N (2014) Microbial degradation of azo dyes: a review. Int J Curr Microbiol App Sci 3:670–690

Takao S (1965) Organic acid production by Basidiomycetes. I. Screening of acid-producing strains. App Microbiol 13(5):732–737

Thao TP, Kao HC, Juang RS, Lan JCW (2013) Kinetic characteristics of biodegradation of methyl orange by *Pseudomonas putida* mt2 in suspended and immobilized cell systems. J Taiwan Inst Chem Eng 44:780–785

Vasdev K (2011) Decolorization of triphenylmethane dyes by six white-rot fungi isolated from nature. J Bioremed Biodegrad 2(5):61–66

Wahyuni S, Suhartono MT, Khaeruni A, Purnomo AS, Asranudin Holilah, Riupassa PA (2016) Purification and characterization of thermostable chitinase from *Bacillus* SW41 for chitin oligomer production. Asian J Chem 28(12):2731–2736

Wahyuni S, Khaeruni A, Purnomo AS (2017) Characterization of mannanase isolated from corncob waste bacteria. Asian J Chem 29(5):1119–1120

Wetzstein HG, Schemer N, Karl W (1997) Degradation of fluoroquinolone enrofloxacin by the brown rot fungus *Gloeophyllum striatum*: identification of metabolites. App Environ Microb 63:4272–4281

Wetzstein HG, Stadler M, Tichy HV, Dalhoff A, Karl W (1999) Degradation of ciprofloxacin by basidiomycetes and identification of metabolites generated by the brown rot fungus *Gloeophyllum* striatum. App Environ Microb 65:1556–1563

Wood PM (1994) Pathways for production of Fenton's reagent by wood-rooting fungi. FEMS Microb Rev 13:313–320

Wu J, Doan H, Upreti S (2008) Decolorization of aqueous textile reactive dye by ozone. Chem Eng J 142:156–160

Yildirim AÖ, Gül Ş, Eren O, Kuşvuran E (2011) A comparative study of ozonation, homogeneous catalytic ozonation, and photocatalytic ozonation for C.I. Reactive Red 194 azo dye degradation. CLEAN Soil Air Water 39(8):795–805

Zeng G, Cheng M, Huang D, Lai C, Xu P, Wei Z, Li N, Zhang C, He X, He Y (2015) Study of the degradation of methylene blue by semi-solid-state fermentation of agricultural residues with *Phanerochaete chrysosporium* and reutilization of fermented residues. Waste Manag 38:424–430

Zhu GC, Shou JX, Qian JW, Xin HZ, Qiu MQ (2014) Degradation of Methylene Blue by Fenton-like reaction. J Adv Mater Res 1065–1069:3127–3130